Seismic Response of Levees in the Sacramento-San Joaquin Delta

Tadahiro Kishida,[a] M.EERI, Ross W. Boulanger,[b] M.EERI, Norman A. Abrahamson,[c] M.EERI, Michael W. Driller,[d] M.EERI, and Timothy M. Wehling,[e] M.EERI

The seismic response of levees in the Sacramento-San Joaquin Delta, where the subsurface soils include thick deposits of highly organic soils, is evaluated. One-dimensional (1-D) and two-dimensional (2-D) equivalent-linear analyses were performed that accounted for variability in ground motions, dynamic properties, and soil profiles. Regression models were developed for: (1) the ratio of spectral accelerations at levee crests computed by 2-D versus 1-D response analyses, (2) stress reduction factors from 1-D site response analyses and seismic coefficient reduction factors for various failure surface depths from the 2-D response analyses, and (3) Newmark sliding block displacements computed for the input NEHRP site D ground motions and the computed seismic coefficient time series. The results of these regression models are compared to those obtained in previous studies involving different soil conditions, geometries, and motions. Newmark sliding block displacement hazard curves were calculated for a representative site in the Sacramento-San Joaquin Delta, and the contributions of various uncertainties to the displacement hazard curves are described. [DOI: 10.1193/1.3157259]

INTRODUCTION

The Sacramento-San Joaquin Delta consists of about 1,700 km of levees along various rivers and sloughs that direct water to San Francisco Bay, and provides water that serves about two-thirds of the population in California. The levees build a complicated channel system that surrounds over 60 islands with ground surface levels below the adjacent waterway levels. Levee failures during an earthquake are a major concern because rapid inundation of the inner islands has the potential to reduce significantly the freshwater supply for California, in addition to damaging the natural habitat, crops and civil infrastructure.

Regional evaluations of seismic risk for the Delta require simplified models for estimating the dynamic response and performance of levees where the subsurface soils include thick deposits of highly organic soils. Evaluating the potential for levee deformations during earthquakes requires evaluating: (1) the potential for triggering of

[a] Graduate Engineer, URS Corporation, 1333 Broadway, Suite 800, Oakland, CA 94612
[b] Professor, University of California, One Shield Avenue., Davis, CA 95616
[c] Pacific Gas and Electric, San Francisco, CA 94177
[d] Senior Engineer, California Dept. of Water Resources, 1416 9th Street, Sacramento, CA 95814
[e] Senior Engineer, California Dept. of Water Resources, 1416 9th Street, Sacramento, CA 95814

Earthquake Spectra, Volume 25, No. 3, pages 557–582, August 2009; © 2009, Earthquake Engineering Research Institute

liquefaction in the saturated loose cohesionless soils within the levees or underlying natural deposits and its consequences, and (2) the potential displacements due to yielding along slip surfaces that extend into the soft sediments and organic soils beneath the levees. There are advantages to evaluating the seismic responses and potential deformations of levees using both equivalent-linear and nonlinear methods at this time. One- and two-dimensional equivalent-linear analyses are expected to provide reasonable estimates of seismic responses up through a range of shaking levels that are important to liquefaction triggering evaluations, can be used in uncoupled approaches to estimating potential slide mass displacements, and can be more easily used in Monte Carlo simulations to study the propagation of certain sources of uncertainty. Two-dimensional nonlinear analyses are expected to provide improved modeling accuracy at very strong shaking levels and can directly simulate levee deformations from yielding soils and liquefaction, which is an important advantage for development of fragility relationships (URS 2008). The combination of equivalent-linear and nonlinear analysis methods provides a basis for evaluating the consistency of the predicted trends and relationships over the range of conditions for which consistency is expected.

In this study, simplified models based on equivalent-linear analysis methods are developed for evaluating the regional seismic performance of levees in the Delta. In a companion paper (Kishida et al. 2009), seismic site effects models for Delta levees were developed using one-dimensional (1-D) equivalent-linear site response analyses with a broad range of input motions, levee soil profiles, and realizations of dynamic properties through Monte Carlo simulations. In the present paper, 2-D equivalent-linear dynamic response analyses for three representative levee cross sections were performed that accounted for variability in ground motions and dynamic properties. A regression model is then developed for the ratio of spectral accelerations at levee crests computed by 2-D versus 1-D response analyses. This 2-D/1-D model is combined with the previously developed 1-D site effects model to produce a site effects model for the transverse response of levees. Regression models for the variation of dynamic stresses with depth were then developed using the stress reduction factors from the 1-D site response analyses (i.e., r_d) and the seismic coefficient reduction factors for various failure surface depths from the 2-D response analyses (i.e., $k_{h,max}/\alpha_{crest,max}$). Regression models were also developed for the Newmark sliding block displacements that were computed for the input NEHRP (2003) site D ground motions and the computed seismic coefficient time series. The differences in the Newmark displacements obtained using these different sets of motions or seismic coefficient time series demonstrate how changes in frequency content affect the Newmark displacement calculation. The results of these regression models for 2-D/1-D response ratios, dynamic stresses versus depth, and Newmark displacements are compared to those obtained in previous studies involving different soil conditions, geometries, and motions. Hazard curves for Newmark sliding block displacements were calculated for a representative site in the Sacramento-San Joaquin Delta, and used to illustrate how uncertainties in yield accelerations, and Newmark sliding block models contribute to the displacement hazards. Limitations in the derived models are discussed.

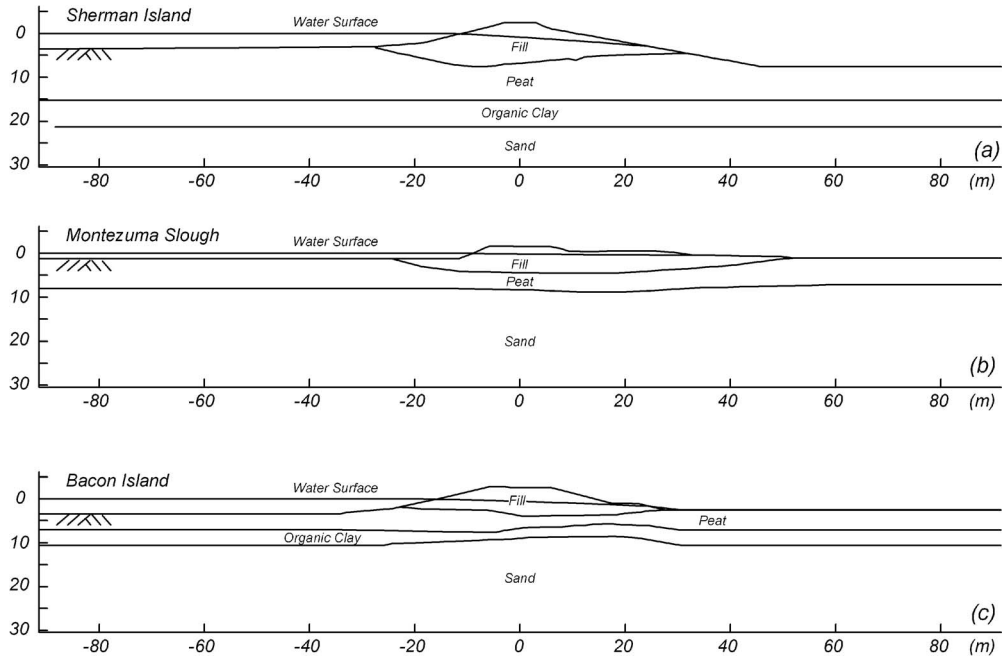

Figure 1. Levee soil profiles at Sherman Island, Montezuma Slough, and Bacon Island.

2-D DYNAMIC RESPONSE ANALYSES

Three representative levee profiles were selected from the Sacramento-San Joaquin Delta for 2-D equivalent-linear dynamic finite element analysis. The levee cross-sections are shown in Figure 1. The fill ranges from 7 m to 11 m thick, while the levee heights range from 2 m to 11 m. The highly organic soil or peat layers range from 2 to 8 m thick beneath the levee fill depending on the location and from 3 m to 12 m thick in the free-field. The peat layers are underlain by organic clay deposits that range from 0 m to 7 m thick. The sand layer beneath the peat and organic clay layers is generally medium-dense to dense with stiff to hard clay interlayers. The slopes of these levees range from about 1V:3.2H to 1V:5.2H on the landward side and from 1V:2.0H to 1V:4.4H on the water side, which is typical of many levees although some levee slopes are locally steeper or flatter than covered by these examples.

Equivalent-linear dynamic finite element analyses for each levee cross-section were performed using the program QUAD4M (Hudson et al. 1994). This finite element program iteratively determines strain-compatible values of shear modulus and damping ratio for each element, and uses Rayleigh damping to achieve the specified damping ratios at two target frequencies (one being the model's fundamental frequency, and the other being a higher frequency that depends on the predominant frequency of the input motion). The effective shear strain for determining strain-compatible properties was taken as 0.65 times the maximum shear strain that occurs during shaking, and the input mo-

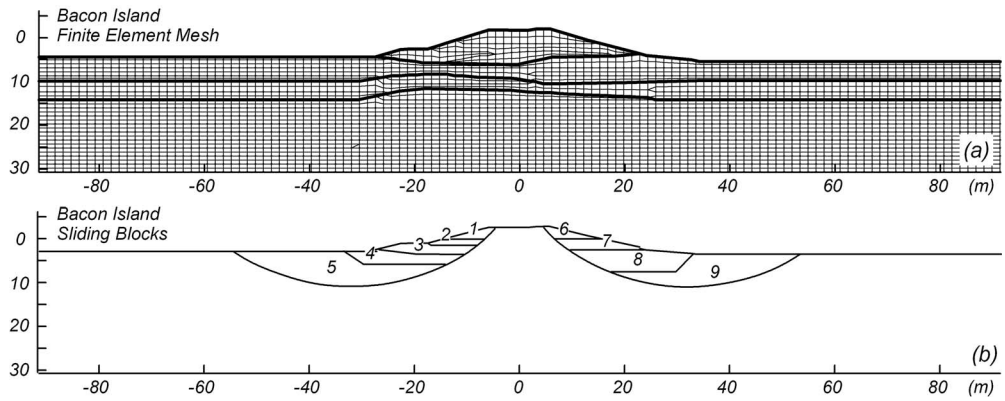

Figure 2. Finite element mesh and sliding blocks at Bacon Island for QUAD4.

tions were specified using the compliant base option. The finite element mesh for a levee on Bacon Island is shown in Figure 2a. For comparison, 1-D site response analyses for the soil profile below the levee crests were performed using the equivalent-linear wave equation analysis method in Shake (Schnabel et al. 1972).

Dynamic properties for the equivalent-linear analysis were estimated based on borehole and in situ test data at these levee locations. Small-strain secant shear modulus (G_{max}) values were estimated using the correlations by Kishida et al. (2008) for peat and organic soils and Kishida (2008) for clay and sand, both of which were calibrated using shear wave velocity data from the Delta and the other locations. Normalized modulus reduction (G/G_{max}) relationships were estimated using the correlations for peat and organic soils by Kishida et al. (2008), for clay by Vucetic and Dobry (1991), and for sand by EPRI (1993). Poisson's ratios were estimated using the relationships by Ishihara (1970). In all cases, the G/G_{max} relationships at large strains were constrained to produce large-strain shear stresses that were consistent with the range of expected strengths for each soil type. Imposing this constraint on G/G_{max} was useful for ensuring that the 1-D Monte Carlo simulation or 2-D dynamic analyses did not inadvertently combine properties that produce unrealistically soft or weak behavior at more moderate strains.

Potential slip surfaces for Newmark sliding block analyses were selected that include wedge failure mechanisms within the levee fills and deep sliding circles through the underlying soft soil and peat deposits. The limit equilibrium program UTEXAS3 (Wright 1990) was used to identify potential deep circular sliding surfaces. Soil strengths were estimated using site-specific data and correlations by Kulhawy and Mayne (1990) and Edil and Wang (2000). The position of the deep circular sliding surfaces were, however, relatively insensitive to the selection of soil strengths. Figure 2b shows the sliding blocks for the levee profile from Bacon Island.

Two hundred and sixty four strong ground motion records from NEHRP site D stations were used as outcrop input motions for the 1-D and 2-D equivalent-linear analyses. These records had peak horizontal accelerations (*PGA*) ranging from 0.004 g to 1.78 g, and were recorded at distances of 1.1 km to 296 km during earthquakes with moment magnitudes (M_w) of 4.3 to 7.9. No scaling or modification of input motions was performed.

Horizontal seismic coefficient time series were determined for each of the potential sliding blocks for each levee cross-section. Newmark sliding block displacements were then calculated for a wide range of yield accelerations for each horizontal seismic coefficient time series.

The results of these 2-D equivalent-linear analyses are expected to be reasonably accurate up to moderate shaking levels, after which the limitations of the equivalent-linear model will progressively become more significant. The equivalent-linear analyses were nonetheless performed for a broad range of shaking levels so that trends in the results were well developed, with the recognition that the results should be complemented by nonlinear analyses for the evaluation of levee performances (e.g., URS 2008).

2-D/1-D RATIOS OF LEVEE CREST RESPONSE

Linear-elastic, 5%-damped, response spectra were computed for the motions at the center of the levee crest from the 1-D and 2-D dynamic response analyses, and then the 2-D/1-D ratios (or correction factors, CF) of spectral values for the identical soil profiles through the center of the levee crests were determined as follows:

$$CF(T) = \frac{Sa(T)_{crest,2D}}{Sa(T)_{crest,1D}} \tag{1}$$

Figure 3 shows the variation of the 2-D/1-D correction factor for PGA (i.e., $CF(0)$) against various characteristics of the levee crest motions computed by 1-D analyses, the earthquake magnitude, and the distance. Figures 3a and 3b show that $CF(0)$ is approximately constant with a median value of 1.19 against the levee crest PGA and Sa(0.2) by 1-D analyses, which suggests that nonlinearity in the 2-D analyses is comparable to that in the 1-D analyses. However, there are positive trends in $CF(0)$ against $Sa(1.0)$ shown in Figure 3c and against spectral ratio S_1 shown in Figure 3d; the spectral ratio S_1, defined as

$$S_1 = Sa(1.0)/Sa(0.2) \tag{2}$$

is an index of spectral shape that is approximately independent of PGA (Kishida et al. 2008b). Positive trends were also observed in $CF(0)$ against earthquake magnitude and distance shown in Figures 3e and 3f. These positive trends in $CF(0)$ are all related to an increase in low frequency content relative to the high frequency content in the input motions.

The following model was developed for the 2-D/1-D correction of spectral accelerations after considering numerous possible predictor variables:

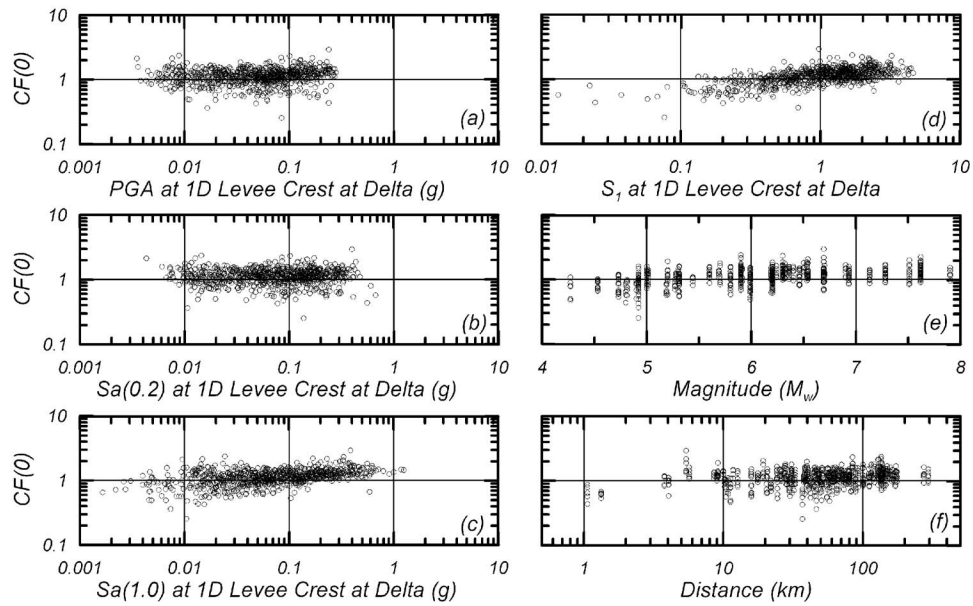

Figure 3. Variation of 2-D/1-D PGA correction against (a) 1-D PGA, (b) 1-D Sa(0.2), (c) 1-D Sa(1.0), (d) 1-D Sa(1.0)/Sa(0.2) (e) magnitude, (f) distance.

$$\ln(CF) = b_0 + b_1 \ln(S_1) \tag{3}$$

Regression results and correlations between residuals are shown in Tables 1 and 2, respectively. The effect of S_1 was significant at short periods, but became insignificant at long periods (e.g., $b_1 = 0$ for periods longer than 1.0 s). The mean value of the 2-D/1-D correction factor for PGA ($CF(0)$) ranges from 0.93 to 1.51 for S_1 values of 0.3 to 3.0. At $S_1 = 1.0$, the plus or minus one standard deviation values for $CF(0)$ are 0.96 and 1.48. Note that the mean value of $CF(0)$ was 1.19 if S_1 was not included in the model. Figure 4 shows the variation of residuals for Equation 3 against different predictor variables. The positive trends in $CF(0)$ against $Sa(1.0)$, magnitude and distance shown in Figure 3 were removed by including S_1 in the regression model.

Table 1. Parameters of 2-D/1-D corrections factors, CF(T)

T (sec)	b_0	b_1	σ
0	0.179	0.213	0.215
0.2	0.099	0.208	0.200
1.0	0.493	0	0.240
5.0	0.171	0	0.209

Table 2. Correlations between residuals of CF(T)

T (sec)	0	0.2	1.0	5.0
0	1	0.51	0.46	0.26
0.2	0.51	1	0.23	0.20
1.0	0.46	0.23	1	0.39
5.0	0.26	0.20	0.39	1

Site dependent variability in the 2-D/1-D correction factors was found to be negligible compared to the variability in the predicted 1-D site response. The random effects in $CF(0)$ between the three levee profiles analyzed (Figure 1) were less than 28% of the variance in $CF(0)$ and only about 13% of the variance in the 1-D site effects models developed for the Delta by Kishida et al. (2008b). Obtaining an accurate estimate of the random effects between levee profiles would require a significantly larger number of levees, but these initial results suggest that the effects of levee geometry are a relatively small source of uncertainty relative to the uncertainties in the outcrop motion, 1-D site response, and 2-D/1-D correction factors excluding the portion attributed to the random effect of levee geometry. For example, this estimate of the random effects from levee geometry would only increase the standard deviation in $Sa(0)$ at a levee crest by 5%.

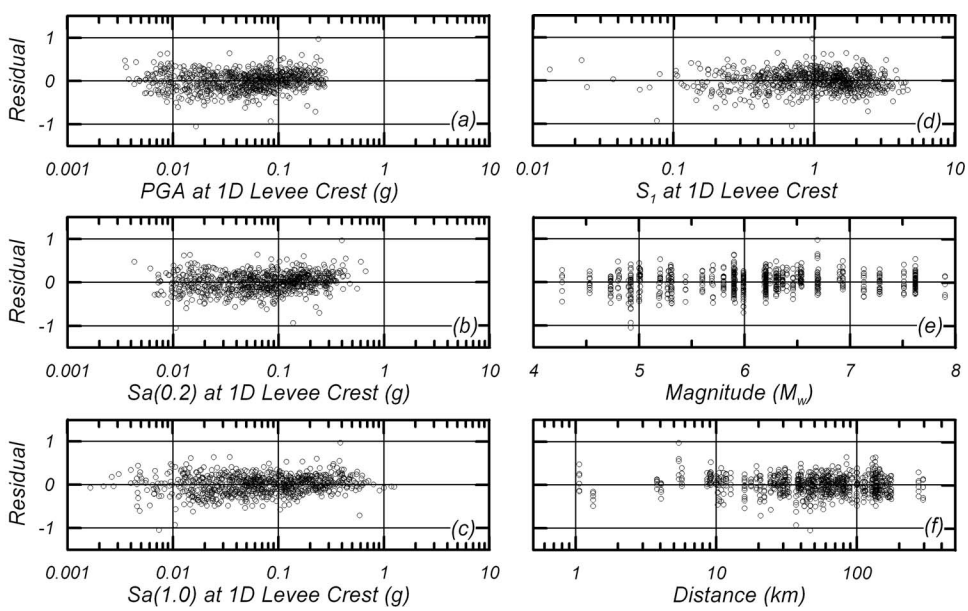

Figure 4. Variation of residuals for 2-D/1-D PGA correction against (a) 1-D PGA, (b) 1-D Sa(0.2), (c) 1-D Sa(1.0), (d) 1-D Sa(1.0)/Sa(0.2), (e) magnitude, (f) distance.

Other studies have compared 2-D and 1-D dynamic response analysis results for various types of embankments and slopes. For example, the 2-D/1-D correction factor of peak crest acceleration was 1.25 for the moderately steep slopes of landfills (Rathje and Bray 2001) and approximately 1.5 for steep hillside slopes in weakly cemented granular soils (Ashford and Sitar 2002). Levees in the Delta typically have gentler slopes than were used in those prior studies, which suggest that median 2-D/1-D correction factors for the Delta would be expected to be smaller, although the significant differences between landfills, cemented sand slopes, and levees mean that the results may not be directly comparable. The levees are also often underlain by thick deposits of soft soils that can have a stronger effect on the natural periods of a levee than changes in side slopes sometimes have. For this study, it was concluded that the dynamic response of levees could be reasonably estimated by combining the 1-D site effects models by Kishida et al. (2009) with the 2-D/1-D correction factor of Equation 3.

STRESS REDUCTION AND SEISMIC COEFFICIENTS

Regression models for estimating dynamic stresses versus depth within a levee were developed using stress reduction factors (r_d) from the 1-D site response analyses and seismic coefficient reduction factors ($r_{2\text{-D}}$) from the 2-D response analyses. The 1-D stress reduction factor, introduced by Seed and Idriss (1971), relates the maximum dynamic stress (τ_{max}) at depth to the maximum stress that would have occurred if the soil column had acted as a rigid body under the maximum horizontal acceleration at the ground surface.

$$r_d = \frac{\tau_{\max} g}{\sigma_{vo} a_{crest,\max}} \tag{4}$$

The seismic coefficient reduction factor ($r_{2\text{-D}}$) from 2-D analyses relates the maximum horizontal seismic coefficient ($k_{h,max}$) for a potential slide mass to the maximum horizontal acceleration at the center of the levee crest as

$$r_{2D} = \frac{k_{h,\max} g}{a_{crest,\max}} \tag{5}$$

The horizontal seismic coefficient time series is determined as

$$k_h(t) = \frac{F(t)}{Mg} \tag{6}$$

where F is the total horizontal seismic force acting on the potential sliding block of mass, M. The definition of $r_{2\text{-D}}$ is equivalent to that of r_d for the case of a horizontal slide plane beneath a level ground surface.

1-D STRESS REDUCTION FACTORS

A data set of stress reduction factors (r_d) was compiled from the 1-D equivalent-linear site response analyses performed by Kishida et al. (2009). Those analyses in-

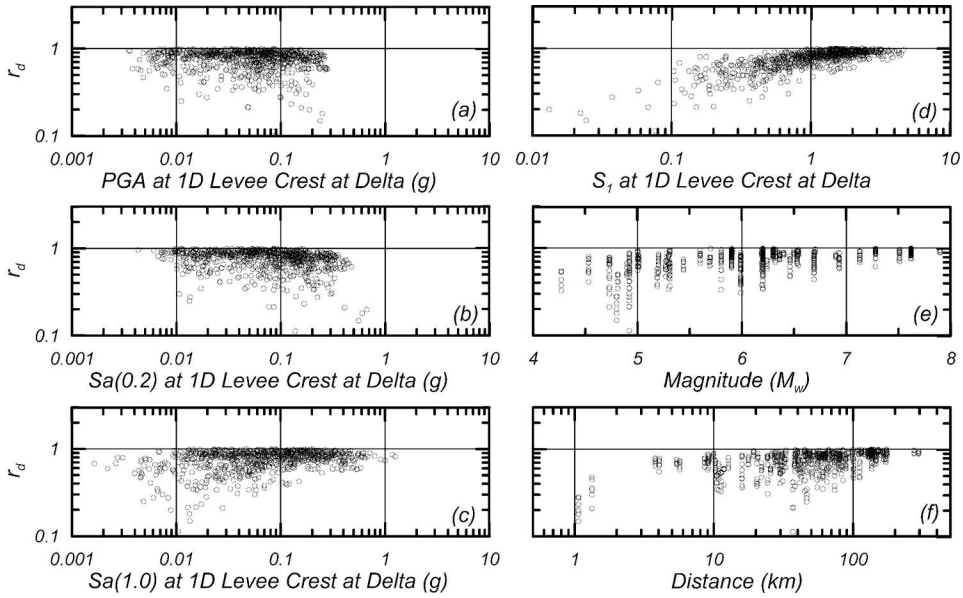

Figure 5. Variation of r_d from the depth of 7.5 to 10 m.

cluded eighteen soil profiles with average shear wave velocities from the surface to a depth of 20 m that ranged from 110 m/s to 190 m/s, 264 input motions from NEHRP site D outcrops, and five simulations of dynamic properties at each soil profile through Monte Carlo simulations. Figure 5 shows the variation of r_d between depths from 7.5 m to 10 m against the earthquake magnitude, distance, and characteristics of the ground surface motion. Figures 5a and 5b show that r_d slightly decreases with increasing PGA or $Sa(0.2)$, which may be related to the soils becoming more nonlinear at stronger shaking levels or the effects of increasing high frequency content; both effects would cause wave lengths to be shorter, such that seismic stresses would reduce more quickly with depth. Figures 5c–5f show that r_d tends to increase with increasing $Sa(1.0)$, S_1, M_w and distance, with the trend against S_1 being the clearest. These trends are all related to the effects of increasing the low frequency content in the input ground motions, which causes wavelengths to be longer and thus the seismic stresses to reduce more slowly with depth.

A regression model for r_d was developed based on superimposing the theoretical response of a soil column to two largely-independent frequencies and incorporating S_1 as a variable.

$$r_d(z) = \left[\frac{1}{2} \left(\frac{\sin \frac{\pi}{2} \frac{T'_S}{0.2}}{\frac{\pi}{2} \frac{T'_S}{0.2}} + \frac{\sin \frac{\pi}{2} \frac{T'_S}{1}}{\frac{\pi}{2} \frac{T'_S}{1}} \right) \right]^a + \frac{b_2}{2} \frac{1 - S_1}{1 + S_1} \left(\frac{\sin \frac{\pi}{2} \frac{T'_S}{0.2}}{\frac{\pi}{2} \frac{T'_S}{0.2}} - \frac{\sin \frac{\pi}{2} \frac{T'_S}{1}}{\frac{\pi}{2} \frac{T'_S}{1}} \right) \tag{7}$$

where

$$T'_S(z) = \min\left(\frac{4z}{\bar{V}_S}, 0.6s \right) \tag{8a}$$

$$a = b_0 PGA^{b_1} \tag{8b}$$

The parameter $\bar{V}_S$ is the average shear wave velocity from the ground surface to a depth, z, and the parameter T'_S is the natural period of the soil column above depth z but with a maximum value of 0.60 sec. In Equation 7, the first term is affected by the intensity of shaking through the exponent term given by equation 8b, and the second term is affected by the frequency content of the input motion through the parameter S_1. The model was regressed against the data after applying the following transformation:

$$\ln(1 - r_d) = \ln(1 - r_{d_Eq7}) + \varepsilon \tag{9}$$

where ε follows the normal distribution with standard deviation of σ. The stress reduction factor is then computed as follows:

$$r_d = E[r_d] + (1 - e^{\varepsilon})(1 - E[r_d]) \tag{10}$$

The regression analyses produced b_0=0.651, b_1=0.0473, b_2=0.833, and σ=0.521.

The residuals of the r_d model are plotted against predictor variables in Figure 6. The residuals have a slightly negative bias for natural soil column periods between 0.25 and 0.5 sec (i.e., between depths of about 6 and 12 m), which means that the model would slightly underestimate r_d at these depths. However, none of the trends were considered significant enough to warrant increasing the complexity of the model.

The variation of r_d versus depth, as predicted by the regression model, is shown in Figure 7 for three cases: Figure 7a shows how r_d increases with increasing S_1, Figure 7b shows how r_d is only very slightly reduced by increasing PGA, and Figure 7c illustrates the uncertainty in r_d by plotting the plus and minus one standard deviation values. The r_d tends to increase with the increase of S_1 due to the increase of low frequency content (producing longer wave lengths), and decrease with increase of PGA due to the nonlinear behavior of soils (producing lower secant shear modulus and hence shorter wave lengths).

The r_d regression model is compared in Figure 8 to the models proposed by Cetin et al. (2004) and Idriss (1999) for six different cases. These six cases correspond to soil profiles with uniform shear wave velocities of 100 m/s or 160 m/s subjected to earthquakes of magnitude 5.5, 6.5, or 7.5. The PGA is 0.2 g in all six cases, and median val-

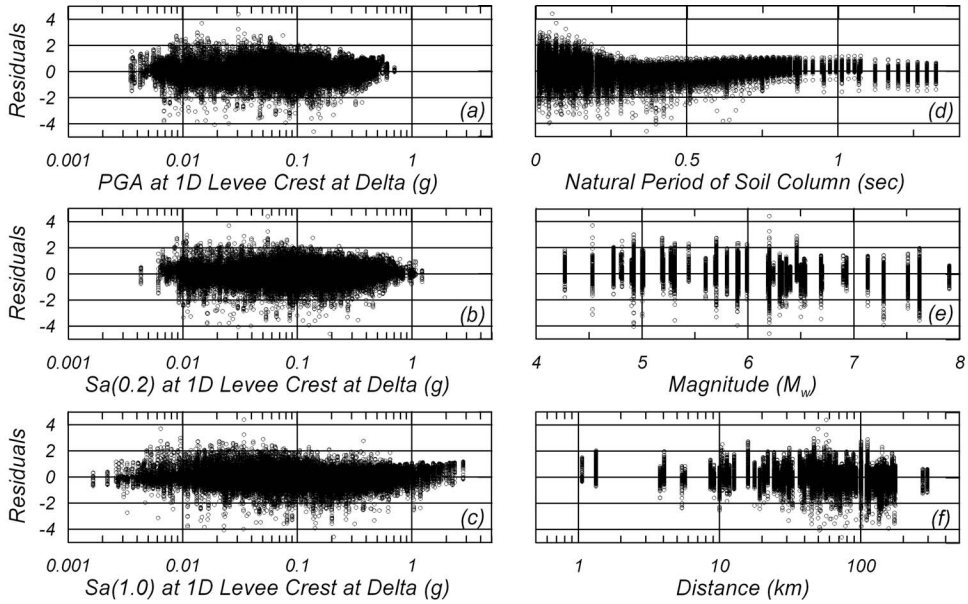

Figure 6. Variation of residuals of maximum stress reduction factor, r_d.

ues of S_1 were estimated for each PGA and magnitude pair. The r_d values by Cetin et al. (2004) are lowest for all six cases. The r_d values by Equation 7 are lower than those by Idriss (1999) when V_s of 100 m/s is used (Figures 8a, 8c, and 8e), but similar to those by Idriss (1999) when V_s of 160 m/s is used (Figures 8b, 8d, and 8f). These differences between Equation 7 and Idriss (1999) were expected because the model by Idriss (1999) was developed more for sandy soil profiles, for which the higher V_s values are more typical. The r_d values by Equation 7 and Idriss (1999) do not drop as quickly with depth as do the Cetin et al. (2004) values and they remain higher at all depths for M of 5.5, 6.5, or 7.5. The reasons why the Cetin et al. (2004) values are significantly lower than obtained by Equation 7 are not clear, however.

2-D SEISMIC COEFFICIENT REDUCTION FACTORS

Seismic coefficient reduction factors ($r_{2\text{-D}}$) from the 2-D dynamic analysis were determined for seventeen different sliding blocks from the three levee profiles (Figures 1 and 2) with 264 ground motions. The values of $r_{2\text{-D}}$ from the deep circular failure mechanisms on both sides of the three levee cross-sections (total of six slide masses) are shown in Figure 9. Figures 9a and 9b show a very small trend of decreasing $r_{2\text{-D}}$ with increasing PGA and $Sa(0.2)$, which may be related to the nonlinear behavior of the soils or the effects of increasing high frequency content. Figures 9d–9f show a trend of increasing $r_{2\text{-D}}$ with increasing S_1, M_w, and distance. These trends are the same as those observed in the 1-D analysis results (Figure 5), with the trend against S_1 again being stronger than for M_w and distance.

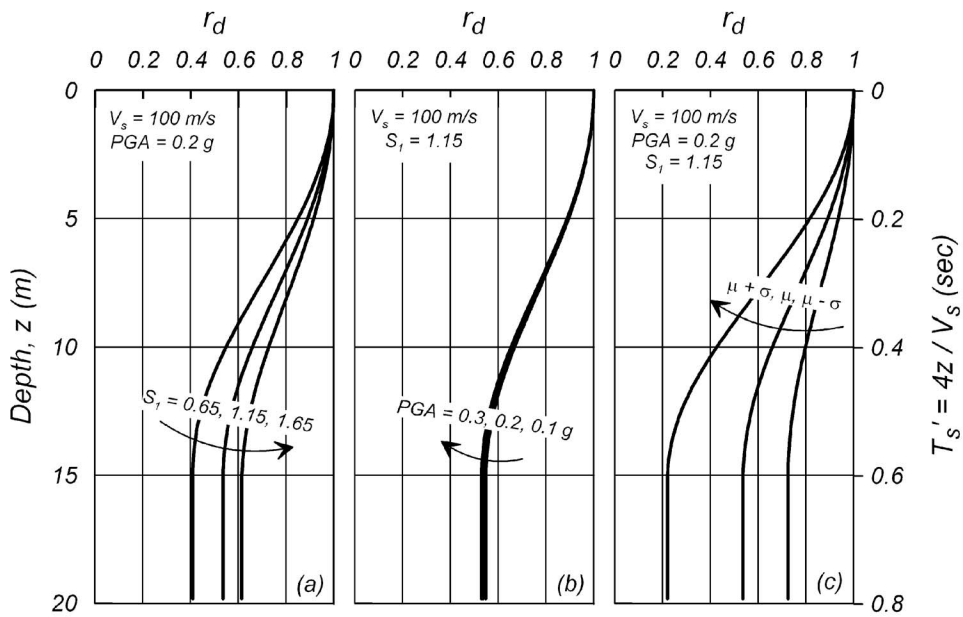

Figure 7. One dimensional stress reduction factor at Delta showing (a) the effect of S_1 on r_d; (b) the effect of PGA on r_d; and (c) the uncertainty in r_d by plotting the plus and minus one standard deviation values.

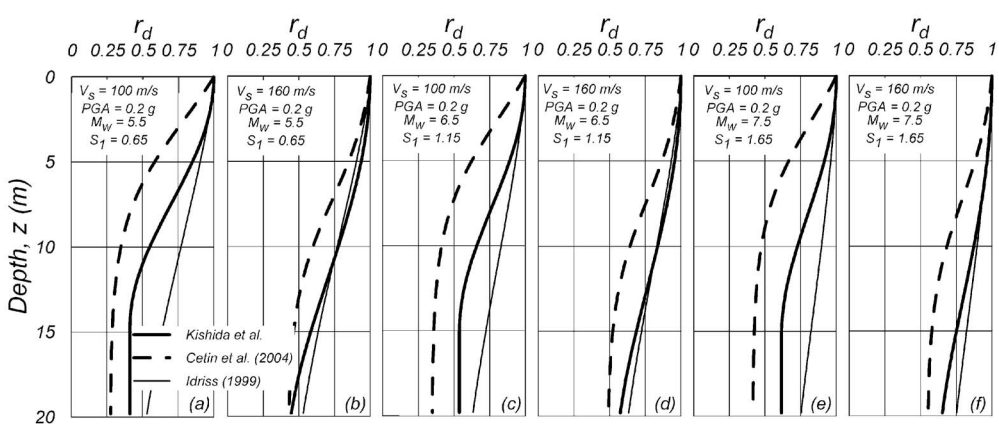

Figure 8. Comparison of stress reduction factor of r_d with different M_w and V_s.

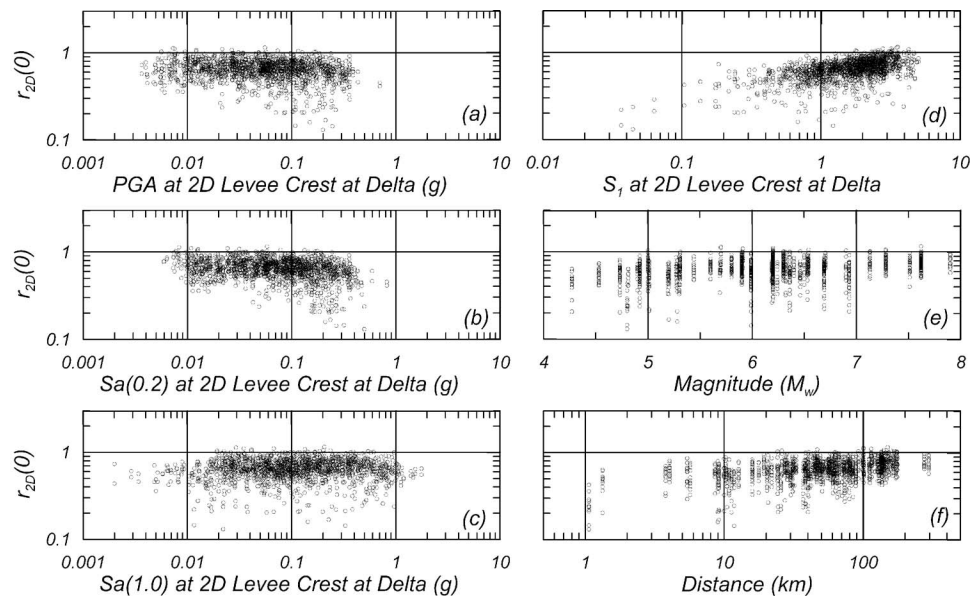

Figure 9. Variation of $k_{h,max}/PGA_{crest,2\text{-}D}$ for deep sliding blocks against (a) PGA at 2-D levee crest, (b) Sa(0.2) at 2-D levee crest, (c) Sa(1.0) at 2-D levee crest, (d) S_1 at 2-D levee crest, (e) magnitude, (f) distance.

A regression model for $r_{2\text{-D}}$ of each sliding block was developed as a function of S_1 as

$$r_{2D} = b_0 + b_1 S_1 + \tau \tag{11}$$

where S_1 is the spectral ratio $Sa(1.0)/Sa(0.2)$ at the center of levee crest, and τ is the fixed effect assigned to each sliding block. The purpose of this regression model is to find the expected response for each block at specified values of S_1, after which the expected $r_{2\text{-D}}$ values can be compared to the previously derived 1-D r_d model. Figure 10a shows the $r_{2\text{-D}}$ regression results against depth (from levee crest to the bottom of the sliding surfaces), with the 1-D r_d model shown for comparison. The $r_{2\text{-D}}$ values are reasonably approximated by the 1-D r_d model, although the 1-D model slightly underestimates the seismic coefficients for sliding blocks near the levee crest edges because the edges of the levee crest have higher accelerations than the center of the levee crest.

The residuals of the 2-D seismic coefficient reduction factors relative to the values predicted by the 1-D r_d model are plotted against predictor variables in Figure 11. These residuals, which are defined as

$$\varepsilon = r_{2D} - E[r_d] \tag{12}$$

are distributed against predictor variables with a standard deviation of 0.20. There is a small nonlinear trend against spectral accelerations at the levee crest, as shown in Fig-

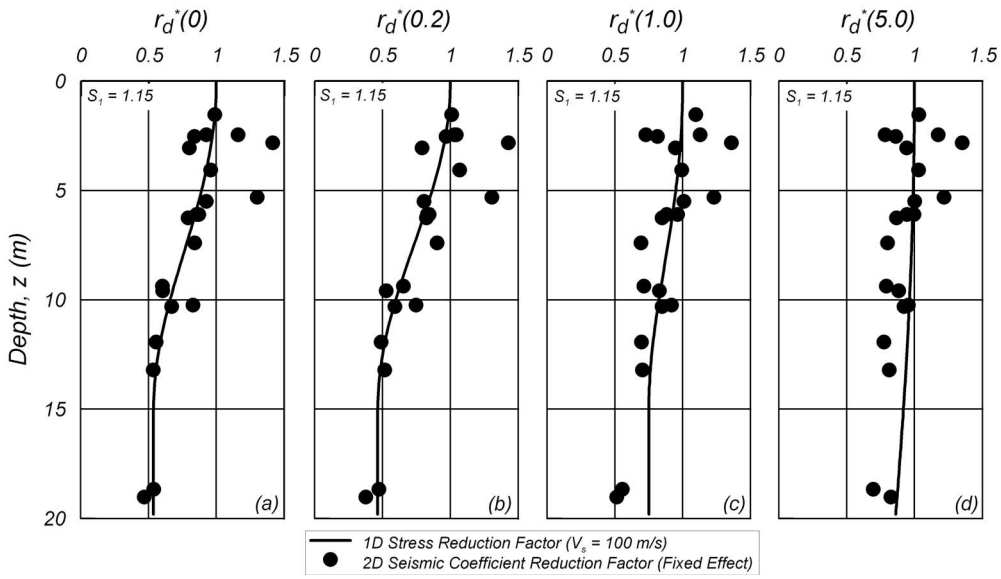

Figure 10. Comparison of seismic coefficient reduction from 2-D analyses to stress reduction factor from 1-D analysis with PGA of 0.2 g for three levees.

ures 11a–11c, but the trends are small enough to be neglected. There are no significant trends against depth, magnitude, or distance, which indicates that the strong effects that these variables have on 2-D seismic coefficients (Figures 9 and 10) are adequately accounted for by the 1-D r_d model (Equation 7).

FREQUENCY CONTENT IN DYNAMIC STRESSES FROM 1-D AND 2-D ANALYSES

The seismic coefficients for potential sliding surfaces at various depths in a levee will vary not just in their peak values, but also in their frequency contents. Differences in frequency content of seismic coefficients or acceleration time series can affect the sliding block displacement calculated by coupled or uncoupled Newmark (1965) type procedure. The differences in how frequency content varied with depth of sliding surface are discussed in this section, and their effects on the Newmark sliding block displacements are evaluated in the subsequent section.

The effect of depth on the frequency content of the 1-D dynamic stresses and 2-D seismic coefficients was evaluated by generalizing the definitions of r_d and $r_{2\text{-D}}$ in terms of spectra values for the equivalent rigid-body accelerations. The generalized 1-D stress reduction factor (r_d^*) was defined as

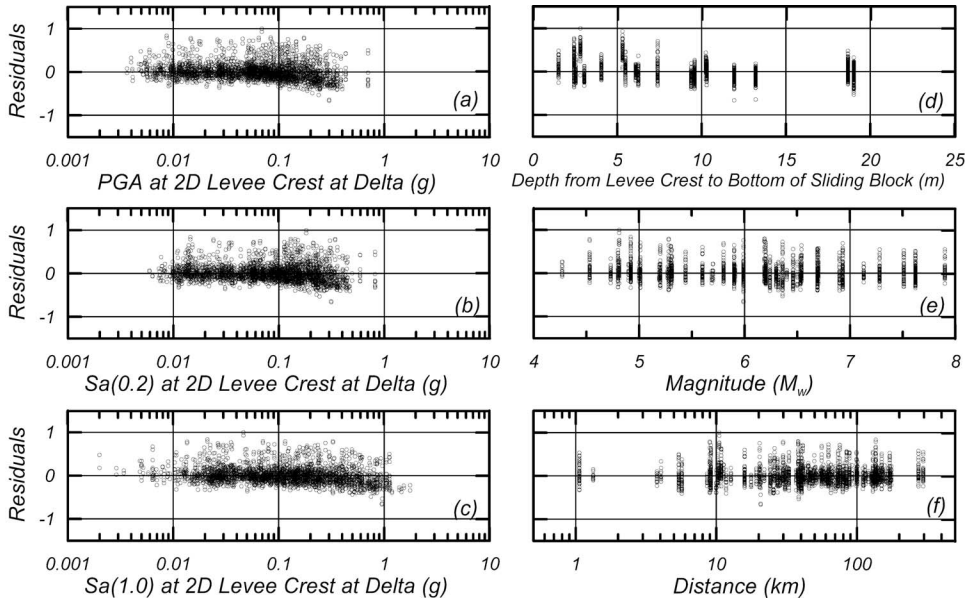

Figure 11. Variation of residuals of seismic coefficient reduction factors from 2-D analyses against variables.

$$r_d^*(T) = \frac{Sa(\tau/\sigma_{vo}, T)}{Sa(a_{crest,1D}/g, T)} \tag{13}$$

where $Sa(\tau/\sigma_{vo}, T)$ is the response spectra for the time histories of shear stress (τ) divided by total stress (σ_{vo}) at a given depth, and $Sa(a_{crest,1\text{-}D}, T)$ is the response spectra for the surface acceleration time series. The generalized 2-D seismic coefficient reduction factor (r_{2D}^*) was similarly defined as

$$r_{2D}^*(T) = \frac{Sa(k_h, T)}{Sa(a_{crest,2D}/g, T)} \tag{14}$$

where $Sa(k_h, T)$ is the response spectra for the seismic coefficient time series.

Regression models for r_d^* and r_{2D}^* were developed for periods of 0 sec, 0.2 sec, 1.0 sec, and 5.0 sec. For periods of 0 sec, 0.2 sec, and 1.0 sec, the same function form as used for r_d and $r_{2\text{-}D}$ were used (i.e., Equation 7). For a period of 5.0 sec, the functional form for r_d was modified so that it better represented the transmission of longer period components of motion, as,

$$r_d^* = \left(\frac{\sin \frac{\pi}{2} \frac{T_S}{5}}{\frac{\pi}{2} \frac{T_S}{5}} \right)^a \tag{15}$$

but with the same form for the exponent "a" from Equation 8b. The results for r_d^* and r_{2D}^* at periods of 0, 0.2, 1.0, and 5.0 sec are shown in Table 3 and plotted versus depth in Figures 10a–10d, respectively, showing that the longer-period components of the ground motions (and dynamic stresses) decrease more slowly with depth below the ground surface than do the short period components (including the PGA). This effect is expected because the longer period components of motion have longer wave lengths.

NEWMARK SLIDING BLOCK DISPLACEMENT

Newmark sliding block displacements were calculated for the seismic coefficient time series from the 17 sliding blocks from the three levee profiles for all 264 input ground motions recorded at NEHRP site D stations. For comparison, sliding block displacements were also calculated for more than 3500 acceleration time series from NEHRP site D stations in the PEER (Pacific Earthquake Engineering Research) NGA database (PEER 2005). Yield accelerations (k_y) for the sliding blocks for both data sets were varied from k_y/PGA of 0.005 to 0.95.

Regression models for the Newmark sliding block displacements were developed using the functional form by Saygili and Rathjie (2008). The first regression model used only k_y and PGA (or k_y and $k_{h,\max}$ for the seismic coefficient data set) as predictor variables:

$$\ln(D) = a_1 + a_2\left(\frac{k_y}{PGA}\right) + a_3\left(\frac{k_y}{PGA} - 0.2\right)^2 + a_4\left(\frac{k_y}{PGA} - 0.2\right)^3 + a_5\left(\frac{k_y}{PGA} - 0.2\right)^4 + a_6 \ln(PGA) \tag{16}$$

where D is the displacement in centimeters. The residuals for this model showed positive trends against M_w, distance, and S_1. Revised regression models with M_w and S_1 as predictive variables were subsequently evaluated.

Table 3. Parameters for 1-D stress reduction factors, $r_d^*(T)$

T (sec)	b_0	b_1	b_2	σ
0	0.651	0.0473	0.833	0.521
0.2	0.824	0.0441	0.856	0.477
1.0	0.276	0.111	0.0482	0.672
5.0	15.6	0.0446		1.25

$$\ln(D) = a_1 + a_2\left(\frac{k_y}{PGA}\right) + a_3\left(\frac{k_y}{PGA} - 0.2\right)^2 + a_4\left(\frac{k_y}{PGA} - 0.2\right)^3 + a_5\left(\frac{k_y}{PGA} - 0.2\right)^4 + a_6 \ln(PGA) + a_7 M_w \tag{17}$$

$$\ln(D) = a_1 + a_2\left(\frac{k_y}{PGA}\right) + a_3\left(\frac{k_y}{PGA} - 0.2\right)^2 + a_4\left(\frac{k_y}{PGA} - 0.2\right)^3 + a_5\left(\frac{k_y}{PGA} - 0.2\right)^4 + a_6 \ln(PGA) + a_7 \ln(S_1) \tag{18}$$

Table 4 shows the parameters and standard deviations obtained by the regression models of Equations 16–18 for both the seismic coefficient data set and the NEHRP site D data set. The standard deviations for the models using either M_w or S_1 as a predictor variable were comparable. The model using S_1 has the advantage that the parameter S_1 is not affected by the scaling of acceleration time series, whereas M_w loses some meaning when the acceleration time series is scaled. The residuals for the model using S_1 show no trend against PGA, Sa(0.2), and Sa(1.0), as shown in Figures 12a–12c. However, there continue to be positive trends against Sa(5.0), M_w, distance, and duration (defined by Trifunac and Brady 1975) as shown in Figures 12d and 12f–12h, which suggests that the model does not fully account for the effects of longer period components or duration of shaking.

A fourth regression model was subsequently developed that includes a measure of the longer period components of spectral accelerations. The covariance matrix of PGA, S_1 and $Sa(5.0)$ were obtained as follows based on NEHRP site D recordings in the NGA database:

Table 4. Regression results of Newmark sliding block displacement

	Delta Levee Seismic Coefficient				NEHRP Site D Ground Motions			
	Equation 16	Equation 17	Equation 18	Equation 23	Equation 16	Equation 17	Equation 18	Equation 23
a_1	7.24	0.812	6.20	7.50	5.30	−3.19	6.58	7.37
a_2	−7.22	−7.35	−7.23	−7.24	−9.16	−9.18	−9.17	−9.18
a_3	11.9	12.5	12.1	12.0	15.8	15.4	15.4	15.2
a_4	−28.3	−29.4	−28.6	−28.1	−35.4	−34.0	−34.3	−33.3
a_5	12.0	12.6	12.10	11.6	16.7	15.4	15.7	14.7
a_6	1.01	0.656	0.911	0.768	0.650	0.445	0.837	0.784
a_7		0.827	0.945	1.14		1.25	1.10	0.993
a_8				0.655				0.511
σ	0.933	0.774	0.816	0.499	1.28	0.853	0.781	0.560

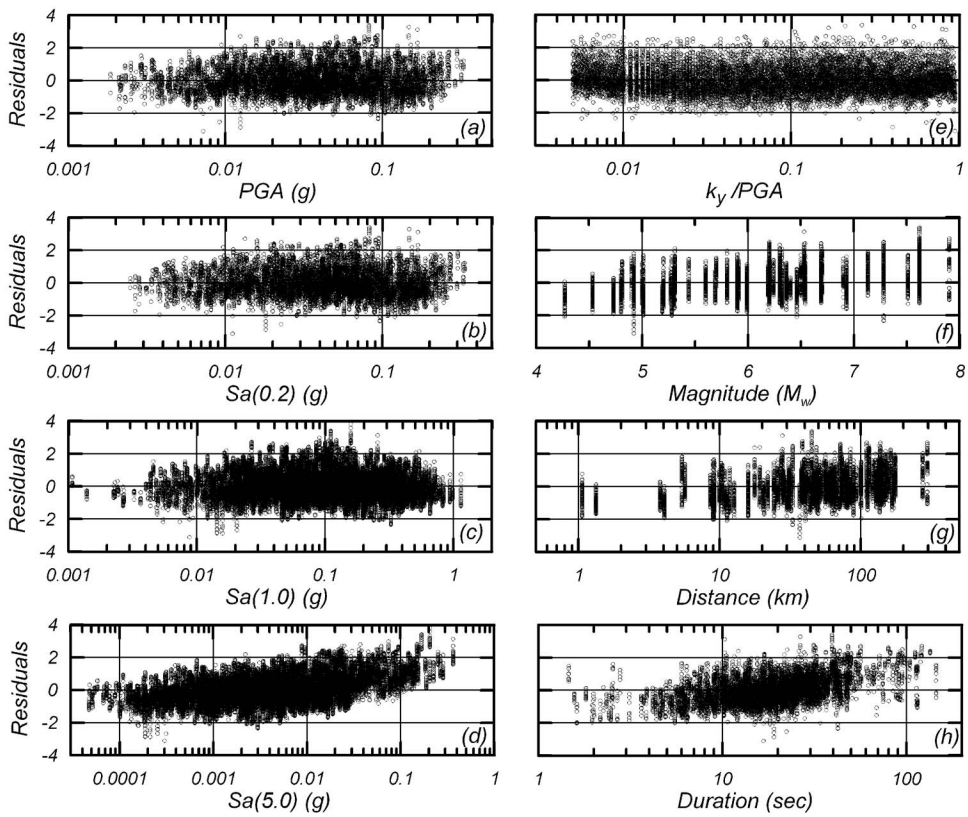

Figure 12. Variation of residuals of Newmark sliding block displacement for the regression model with the predictor variables of k_y/PGA, PGA, and S_1.

$$\Sigma = \begin{bmatrix} 1.182 & -0.196 & 1.089 \\ -0.196 & 0.814 & 0.817 \\ 1.089 & 0.817 & 3.273 \end{bmatrix} \tag{19}$$

The covariance matrix between PGA, S_1, and the linear combination of PGA, S_1, and $Sa(5.0)$ are obtained as follows:

$$\boldsymbol{\Sigma}' = \begin{bmatrix} 1 & 0 & 0 \\ 0 & 1 & 0 \\ a_0 & a_1 & a_2 \end{bmatrix} \begin{bmatrix} 1.182 & -0.196 & 1.089 \\ -0.196 & 0.814 & 0.817 \\ 1.089 & 0.817 & 3.273 \end{bmatrix} \begin{bmatrix} 1 & 0 & 0 \\ 0 & 1 & 0 \\ a_0 & a_1 & a_2 \end{bmatrix}' \tag{20}$$

where the vector $\boldsymbol{a}$ is a unit vector. Since the number of unknown parameters is three, the number of equations with the condition of no correlation is two, and the number of equations for the unit vector is one, the following vectors are obtained:

$$\begin{bmatrix} \ln(PGA) \\ \ln(S_1) \\ \ln(I_1) \end{bmatrix} = \begin{bmatrix} 1 & 0 & 0 \\ 0 & 1 & 0 \\ -0.57 & -0.65 & 0.51 \end{bmatrix} \begin{bmatrix} \ln(PGA) \\ \ln(S_1) \\ \ln(Sa(5.0)) \end{bmatrix} \tag{21}$$

The component $\mathbf{I}_1$ which is independent of PGA and S_1 can be approximated as follows:

$$S_2 = \frac{Sa(0.2) \cdot Sa(5.0)}{PGA \cdot Sa(1.0)} \tag{22}$$

The correlations between S_2 and PGA and between S_2 and S_1 were obtained as 0.09 and 0.21, respectively, which are small enough to be considered as independent. The regression model for Newmark sliding block displacements was then expressed as,

$$\ln(D) = a_1 + a_2\left(\frac{k_y}{PGA}\right) + a_3\left(\frac{k_y}{PGA} - 0.2\right)^2 + a_4\left(\frac{k_y}{PGA} - 0.2\right)^3 + a_5\left(\frac{k_y}{PGA} - 0.2\right)^4 + a_6 \ln(PGA) + a_7 \ln(S_1) + a_8 \ln(S_2) \tag{23}$$

The resulted parameters and the standard deviation are shown in Table 4. The parameters from a_2 to a_6 are relatively stable across all four regression models, which is consistent with the three ground motion characteristics, PGA, S_1, and S_2, being relatively independent of each other. Note that the use of dependent predictor variables such as PGA and Arias Intensity can result in relatively unstable parameter values from regression analyses. The standard deviations for the fourth regression model (Equation 23) were only 0.50 and 0.56 for the two data sets, which are substantially smaller than the values of 0.77 to 1.28 obtained with the first three models.

The residuals from the fourth regression model for Newmark sliding block displacements are plotted against predictor variables in Figure 13. Adding S_2 in the regression model (Equation 18 versus Equation 23) reduced the variance by about 55% and removed the positive trends against $Sa(5.0)$, M_w, distance, and duration that were observed in Figures 12d and 12f–12h. The improvement achieved by including S_2 is partly attributed to the importance of long-period components of motion to sliding block displacements and partly due to the correlation between long-period spectral accelerations and duration of shaking (which are also important to sliding block displacements). For example, the correlation between S_1 and duration was 0.57 and between S_2 and duration was 0.51 for the NEHRP site D ground motion data set. The good performance of this regression model suggests that the addition of S_2 adequately accounted for the effects of both long-period motions and shaking duration.

The dependence of the sliding block regression models on the regression data set is illustrated in Figure 14 showing the attenuation of expected Newmark sliding block displacements with distance from the rupture surface for strike-slip event with M_w=6.5 and with k_y=0.05 g. For this figure, the expected spectral values (which define PGA, S_1, and S_2) were determined using the Abrahamson and Silva (1997) attenuation model for a deep soil site. Figure 14a shows the expected sliding block displacements for the PGA models (Equation 16) and the PGA-M_w models (Equation 17) as calibrated against the

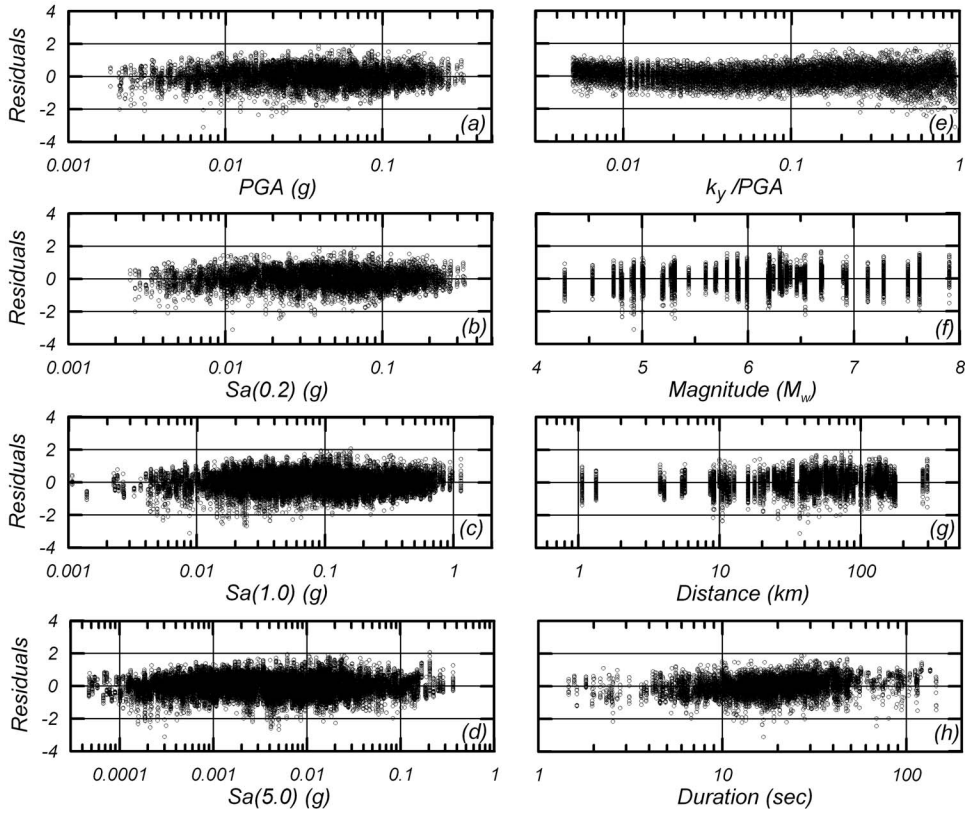

Figure 13. Variation of residuals of Newmark sliding block displacement for the regression model with the predictor variables of k_y/PGA, PGA, S_1, S_2.

seismic coefficient data set or the NEHRP site D data set. The regression models derived from the seismic coefficient data set produced expected displacements that are 3 to 6 times greater than the models derived from the NEHRP site D data set. This indicates that the seismic response of the levees resulted in seismic coefficient time series that differ significantly from the specified input motions (i.e., NEHRP site D outcrop motions) in terms of the characteristics that are important to sliding block calculations (e.g., frequency, phasing, duration). The differences in characteristics between the seismic coefficient time series and the NEHRP site D data sets are not properly captured by the sliding block regression models that rely on *PGA* (or $k_{h,max}$) alone or on the combination of PGA and M_w. Figure 14b shows the expected sliding block displacements for the *PGA*-S_1 models (Equation 18) and the PGA-S_1-S_2 models (Equation 23) as derived from the seismic coefficient data set versus the NEHRP site D data set. The regression models show much smaller differences between the two data sets than were observed

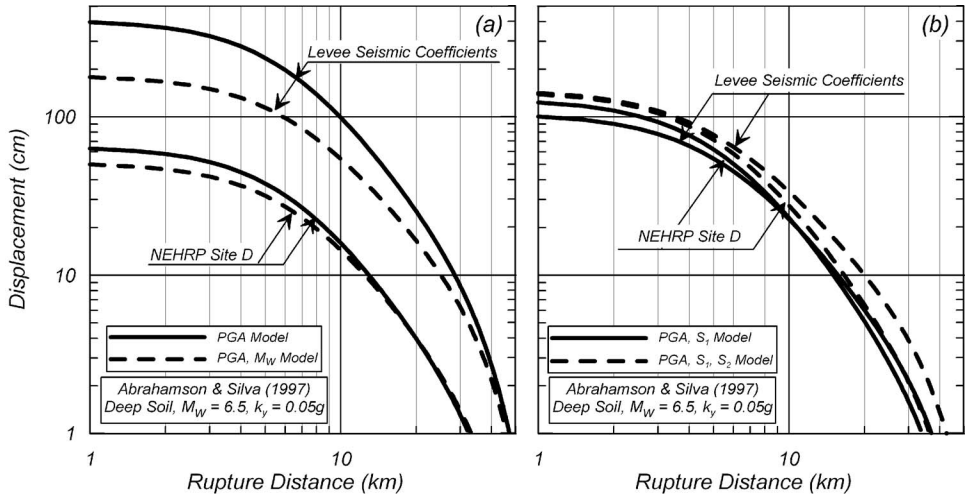

Figure 14. Example of the effect of predictor variables and regression data sets on expected displacement attenuation with distance.

with the PGA or PGA-M_w models, indicating that the S_1 and S_2 predictor variables are reasonably efficient and sufficient for describing the time series characteristic that are important for predicting Newmark sliding block displacements.

The *PGA*-S_1-S_2 regression model is compared to three other models by Bray and Travasarou (2007), Watson-Lamprey (2007), and Saygili and Rathje (2008) in Figure 15 showing the attenuation of expected Newmark sliding block displacements with distance from the rupture surface for strike-slip event with M_w=6.5 and with k_y=0.05 g. For this figure, the expected spectral values (which define *PGA*, S_1, and S_2) were determined using the Abrahamson and Silva (1997) attenuation model for a deep soil site. The differences between the displacements predicted by these four models are attributed to the differences in their predictor variables and the sufficiency of those predictor variables to describe ground motion characteristics important to Newmark sliding block displacements. The predicted displacements by the PGA model by Saygili and Rathje (2008) and *PGA*-M_w model by Bray and Travasarou (2007) tend to saturate faster with decreasing distance than those by the *PGA*-*Sa*(1.0) model by Watson-Lamprey (2007) or PGA-S_1-S_2 model developed herein; this trend is attributed to the former two models having predictor variables that saturate at close distance although the Newmark displacement does not saturate. The role of predictor variables is also illustrated by comparing Figures 14 and 15, and noting that the range of displacements predicted by the PGA, PGA-M_w, PGA-S_1, and PGA-S_1-S_2 models for the NEHRP Site D data set (Figure 14) effectively envelopes the range of displacements predicted by the Bray and Travasarou (2007), Watson-Lamprey (2007), and Saygili and Rathje (2008) models (Figure 15). The four models are, however, reasonably consistent for many practical purposes.

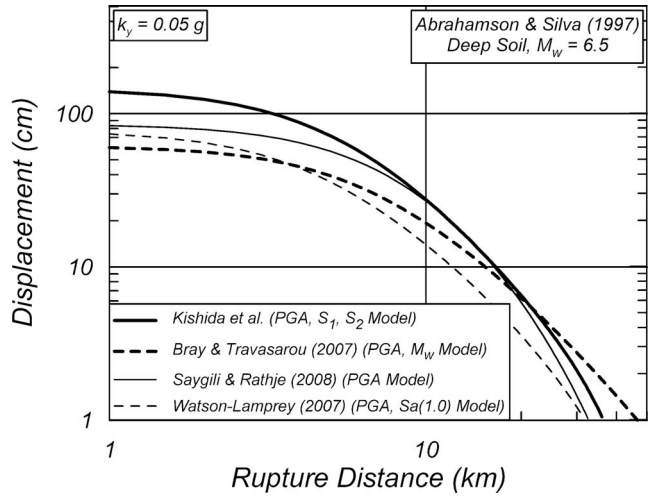

Figure 15. Example illustrating the effect of the Newmark sliding block regression model on the attenuation of expected displacements with distance.

Application of the Newmark sliding block regression models to a levee slope requires estimating the characteristics of the seismic coefficient time series. The site effects model by Kishida et al. (2008b) can be used to estimate the spectral shape of the horizontal accelerations at the levee crest, and the relationships for r_d^* and r_{2D}^* (Equations 20 and 21; Figure 10) can be used to estimate the expected spectral shape of the seismic coefficient time series (e.g., $k_{h,max}$, S_1, S_2). If the Newmark sliding block regression models are used with expected values for the seismic coefficient's characteristics, conditional on the spectral accelerations at the levee crest, then the standard deviations in the predicted displacements increased from 0.93 to 1.07 for the PGA model (Equation 16), from 0.85 to 1.00 for the PGA-M_w model (Equation 17), from 0.82 to 0.97 for the PGA-S_1 model (Equation 18), and from 0.51 to 0.73 for the PGA-S_1-S_2 model (Equation 23).

DISPLACEMENT HAZARD CURVES

Displacement hazard curves for a representative levee site in the Delta with a deterministic k_y=0.1 g were calculated to illustrate the effect of using different Newmark sliding block regression models. Correlations between spectral accelerations were accounted for in the probabilistic hazard analysis using the results of Watson-Lamprey (2008, personal communication) at NEHRP site D, Kishida et al. (2008b) for 1-D site effects, and Table 2 for 2-D/1-D corrections. Figure 16 shows displacement hazard curves computed using the PGA, PGA-S_1, and PGA-S_1-S_2 models. The PGA-S_1 model resulted in the highest displacements, while the PGA-S_1-S_2 model, which is the most sophisticated to implement, resulted in the smallest displacements at mean annual frequencies of exceedance greater than 0.002. The PGA model resulted in intermediate values of displacement at mean annual frequencies of exceedance greater than 0.002. The

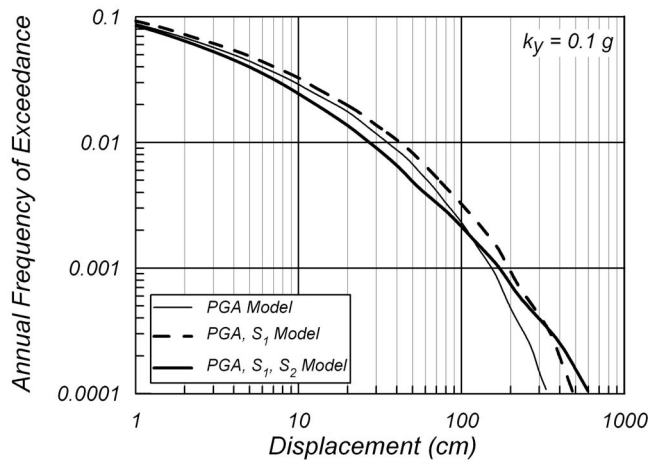

Figure 16. Comparison of displacement hazard curves between PGA, PGA, and S_1, and PGA, S_1, and S_2 model.

differences in displacement hazard can be attributed to: (1) differences in the mean predictions of sliding block displacement for the different combinations of earthquake magnitudes and distances that contribute to the seismic hazard at this location, and (2) differences in the standard deviations for each sliding block regression model. The displacement hazard curves computed using these three models are not, however, significantly different for practical purposes.

Uncertainties in the yield acceleration and Newmark sliding block regression model are both important to the probabilistic calculation of displacement hazards. The role of these uncertainties is illustrated in Figure 17 showing displacement hazard curves obtained using the PGA-S_1-S_2 sliding block regression model, an expected k_y of 0.1 g, and three scenarios regarding the representation of uncertainties. The first case used a deterministic version of the sliding block model (i.e., returns expected values with a standard deviation $\sigma_{dis}=0$) and a deterministic k_y (i.e., $\sigma_y=0$), and resulted in the lowest computed displacement hazard. The second case included the uncertainty in the sliding block model ($\sigma_{dis}=0.73$) while keeping k_y deterministic, and resulted in displacement hazards that were typically about 1.5 times larger than for the first case. The third case included uncertainty in both the sliding block model and k_y (log normal distribution with $\sigma_y=0.4$), and resulted in displacement hazards that were again typically about 1.5 times larger than obtained for the second case. This example illustrates the importance of accounting for the uncertainties in the sliding block model and k_y when performing a probabilistic evaluation of potential slope displacements.

SUMMARY AND CONCLUSION

Regression models for the dynamic response of levees in the Sacramento-San Joaquin Delta were developed based on 1-D and 2-D equivalent-linear dynamic response

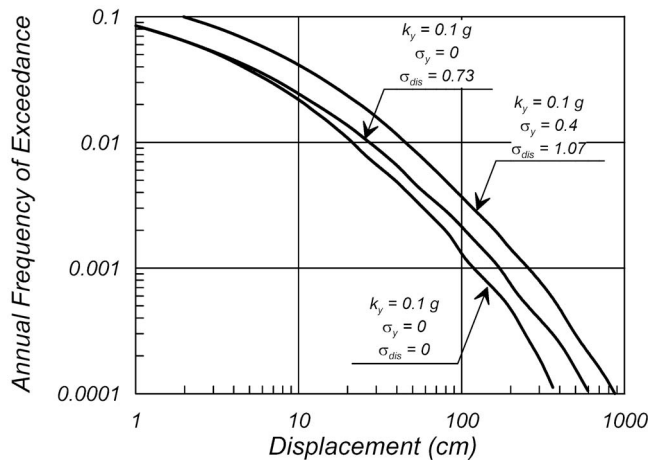

Figure 17. Displacement hazard curves for deep circle slope failure of a levee at Sherman Island with and without inclusion of uncertainty in yield acceleration and Newmark sliding block model.

analyses. The 1-D site effects model (Kishida et al. 2009) was developed based on analyses of 18 representative soil profiles, with five Monte Carlo realizations of dynamic soil properties for each soil profile, subjected to 264 input ground motions. 2-D/1-D correction factors for spectral accelerations at a levee crest were developed herein based on comparisons of 2-D and 1-D dynamic response analyses for three representative levee profiles with 264 input motions. The mean 2-D/1-D correction factor for PGA at a levee crest was approximately 1.19 for all three levee profiles, with the correction factor increasing with increasing low frequency content in the input motion. This 2-D/1-D correction on PGA is considered reasonable given that the levees have relatively gentle slopes and are often underlain by soft sediment layers whose strong influence on levee response is largely approximated by a 1-D model.

Models were also developed for 1-D stress reduction factors (r_d) and 2-D seismic coefficient reduction factors ($r_{2\text{-D}}=k_{h,max}/a_{max,crest}$). The $r_{2\text{-D}}$ results were reasonably approximated by the r_d model when the $r_{2\text{-D}}$ values are plotted against the depth from levee crest to the bottom of the potential failure surface. The model shows increasing r_d values at a given depth for increasing values of V_s and spectral ratio S_1 $(=Sa(1.0)/Sa(0.2))$, but relatively minor effects of PGA.

The regression analyses of the Newmark sliding block displacements showed that combinations of PGA, M_w, and S_1 were insufficient for characterizing the displacements obtained independently from the NEHRP site D acceleration time series and the levee seismic coefficient time series. A regression model based on *PGA*, S_1, and S_2 $(=Sa(5.0)/S_1PGA)$, where S_2 represents the longer period components of motion, was shown to be efficient and sufficient for characterizing Newmark sliding block displacements from either data set.

Hazard curves for Newmark sliding block displacements at a representative levee in the Delta were used to demonstrate the importance of including the uncertainties in both the yield acceleration and the Newmark sliding block regression model. The hazard curves obtained using several different Newmark sliding block regression models were, however, not significantly different which suggests that the simpler models may be adequate for practical purposes.

The regional evaluation of seismic levee performance warrants the judicious use of both equivalent-linear and nonlinear analysis methods to assess the potential for liquefaction triggering and slope deformations across a broad range of conditions. The simplified models presented herein are based on equivalent-linear analyses, and are expected to be reasonably accurate up to moderate shaking levels. Nonlinear analyses should be used to evaluate levee responses at stronger shaking levels and for the direct evaluation of levee deformations (e.g., URS 2008). The collection of strong ground motion recordings on Delta levees remains an important goal for the verification of these different dynamic analysis methods.

ACKNOWLEDGMENTS

This research was supported by the California Department of Water Resources (CDWR), State of California. The views and conclusions contained in this document are those of the authors and should not be interpreted as necessarily representing the official policies, either expressed or implied, of the State of California. The authors appreciate the suggestions and assistance of Dr. Jennie Watson-Lamprey with portions of the analyses. The above support and contributions are greatly appreciated.

REFERENCES

Abrahamson, A. N., and Silva, W. J., 1997 Empirical response spectral acceleration relations for shallow crustal earthquakes, *Seismol. Res. Lett.* **68**, 94–127.

Ashford, S. A., and Sitar, N., 2002. Simplified method for evaluating seismic stability of steep slopes, *J. Geotech. Geoenviron. Eng.* **128**, 119–128.

Bray, J. D., and Travasarou, T., 2007 Simplified procedure for estimating earthquake-induced deviatoric slope displacements, *J. Geotech. Geoenviron. Eng.* **133**, 381–392.

Cetin, K. O., Seed, R. B., Kiureghian, A. D., Tokimatsu, K., Harder, L. F., Kayen, R. E., and Moss, R. E. S., 2004. Standard penetration test-based probabilistic and deterministic assessment of seismic soil liquefaction potential, *J. Geotech. Geoenviron. Eng.* **130**, 1314–1340.

Edil, T. B., and Wang, X., 2000. Shear strength and K_o of peats and organic soils, *Geotechnics of High Water Content Materials*, ASTM STP 1374, American Society for Testing and Materials, 209–230.

Electric Power Research Institute (EPRI), 1993. *Guidelines for site specific ground motions, Rept. TR-102293*, 1-5, Pala Alto, California.

Hudson, M., Idriss, I. M., and Beikae, M., 1994. QUAD4M—A computer program to evaluate the seismic response of soil structures using finite element procedures and incorporation a compliant base, Center for Geotechnical Modeling, Department of Civil and Environmental Engineering, University of California, Davis.

Idriss, I. M., 1999. An update of the Seed-Idriss Simplified Procedure for evaluating liquefaction potential, Presentation notes for Transportation Research Board Workshop on New Approaches to Liquefaction Analysis, held 10 January, Washington, D. C.

Ishihara, K., 1970. Approximate forms of wave equations for water-saturated porous materials and related dynamic modulus, *Soils Found.* **10**, 10–38.

Kishida, T., 2008. Seismic Site Effects for the Sacramento-San Joaquin Delta, Ph. D. thesis, University of California, Davis, in review.

Kishida, T., Boulanger, R. W., Abrahamson, N. A., Wehling, T. M., and Driller, M. W., 2008. Regression models for dynamic properties of highly organic soil, *J. Geotech. Geoenviron. Eng.* **135**, 533–543.

Kishida, T., Boulanger, R. W., Abrahamson, N. A., Driller, M. W., and Wehling, T. M., 2009. Site Effects for the Sacramento-San Joaquin Delta, *Earthquake Spectra* **25**, 301–322.

Kulhawy, F. H., and Mayne, P. W., 1990. *Manual on Estimating Soil Properties for Foundation Design*, EL-6800, Electric Power Research Institute, Palo Alto, CA.

National Earthquake Hazards Reduction Program (NEHRP), 2003. *Recommended provisions for seismic regulations for new buildings and other structures with accompanying commentary*, Building Seismic Safety Council for Federal Emergency Management Agency, Washington, D.C.

Newmark, N. M., 1965. Effects of earthquakes on dams and embankments, *Geotechnique* **15**, 139–160.

Pacific Earthquake Engineering Research Center (PEER), (2005). *Next Generation Attenuation (NGA) Strong Ground Motion Database*, University of California, Berkeley, http://peer.berkeley.edu/nga/index.html

Rathje, E. M., and Bray, J. D., 2001. One- and two-dimensional seismic analysis of solid-waste landfills, *Can. Geotech. J.* **38**, 850–862

Saygili, G., and Rathje., E. M., 2008. Empirical predictive models earthquake-induced sliding displacements of slopes, *J. Geotech. Geoenviron. Eng. ASCE* **134**, 790–803.

Schnabel, P. B., Lysmer, J., and Seed, H. B., 1972. *SHAKE: A computer program for earthquake response analysis of horizontally layered sites*, *Report No. UCB/EERC-2/12*, Earthquake Engineering Research Center, University of California, Berkeley, December, 102pp.

Seed, H. B., and Idriss, I. M., 1971. Simplified procedure for evaluating soil liquefaction potential, *J. Soil Mech. and Found. Div.* **97**, 1249–1274.

Trifunac, M. D., and Brady, A. G., 1975. A study of the duration of strong earthquake ground motion, *Bull. Seismol. Soc. Am.* **65**, 581–626.

URS, 2008. *Delta Risk Management Strategy Phase 1, Risk Analysis Report (Draft 4)*, prepared by URS Corporation/Jack R. Benjamin and Associates, Inc., for California Department of Water Resources, July.

Vucetic, M., and Dobry, R., 1991. Effect of soil plasticity on cyclic response, *J. Geotech. Engrg.* **117**, 89–107.

Watson-Lamprey, J. A., 2007. Selection and Scaling of Ground Motion Time Series, Ph.D. thesis, University of California, Berkeley.

——, 2008. Personal communication.

Wright, S. G., 1990. *UTEXAS3: A computer program for slope stability calculations*, Shinoak Software, Austin, TX.

(Received 5 March 2008; accepted 20 November 2008)